FINAL TECHNICAL REPORT

USGS NEHRP AWARD G10AP00008

January 1, 2010 – December 31, 2010

3D Seismic Velocity Model for the Unconsolidated Mississippi Embayment Sediments from H/V Ambient Noise Measurements

Charles A. Langston

Stephen P. Horton

Center for Earthquake Research and Information
University of Memphis
3876 Central Ave., Suite 1
Memphis, TN 38152-3050

Telephone: (901)-678-4869
Fax: (901) 678-4734
Email: clangstn@memphis.edu

July 19, 2011

ABSTRACT

USGS NEHRP AWARD G10AP00008, *3D Seismic Velocity Model for the Unconsolidated Mississippi Embayment Sediments from H/V Ambient Noise Measurements* by Charles A. Langston and Stephen P. Horton, Center for Earthquake Research and Information, University of Memphis, 3876 Central Ave., Suite 1, Memphis, TN 38152-3050. Telephone: (901) 678-4869, Fax:(901) 678-4734, Email:clangstn@memphis.edu

Nakamura's (1989) H/V technique was applied to data from 29 new field stations and 32 other broadband temporary and permanent seismic stations within the Mississippi embayment of the Central U.S. to develop a three-dimensional model of unconsolidated sediment shear-wave velocity structure. Using Dart's (1992) map of sediment thickness as a basis, a self-consistent model of average shear-wave velocity versus sediment thickness was developed by utilizing the theoretical linear relationship between the frequency of the H/V peak and shear-wave velocity. Although period of the H/V peak versus sediment thickness is seen to be approximately linear, peak frequency, f_P, versus sediment thickness, h, is distinctly non-linear and is parameterized to follow $\ln f = 1.038 \times 10^{-6} h^2 - 0.0026411h + 0.10108$ giving $v_s = 4he^{\ln f}$. This relationship breaks down for h < 200 m where H/V determinations show large scatter. The velocity model is linearly extended to 50 m thickness with a low velocity of 300 m/s specified for less sediment thickness. Overall, the model shows low average shear-wave velocity near the edge of the Mississippi embayment with velocities increasing with increasing sediment thickness, consistent with increased sediment compaction.

INVESTIGATIONS UNDERTAKEN

This project was seismological in scope and involved the collection, processing, and interpretation of an ambient noise data set to develop models of shear wave velocity for unconsolidated sediments of the Mississippi embayment. Table 1 outlines the research program. New ambient noise data were collected for 29 sites during several field campaigns in late Fall 2010 and Spring 2011 (Figure 1). Other seismic data used in this study were available from the IRIS data archives and archives of the New Madrid Cooperative Seismic Network at CERI.

Data Collection (available from archives)
• *Broad band temporary deployments associated with the Embayment Seismic Excitation Experiment (ESEE) in 2002* • *Broad band temporary array experiments in 2002, 2006, 2007, 2008, 2009* • *NM Cooperative Network Broadband data*
• *Regional Broad band stations (IRIS data center)*
• *Download NOAA WaveWatch III models from website*
Data Collection (Field Work)
• *Broad band ambient noise measurements at 26 sites (Figure 1)*
Data Processing
• *H/V resonance period determination*
Data Modeling/Interpretation
• *Produce average shear wave velocity model from H/V analysis and sediment thickness map* • *Produce map of long period resonance period for embayment* • *Produce map of long period amplification at resonance period for embayment* • *Develop vertically inhomogeneous 3D velocity model using well log information*

Table 1 – Summary of the Research Program

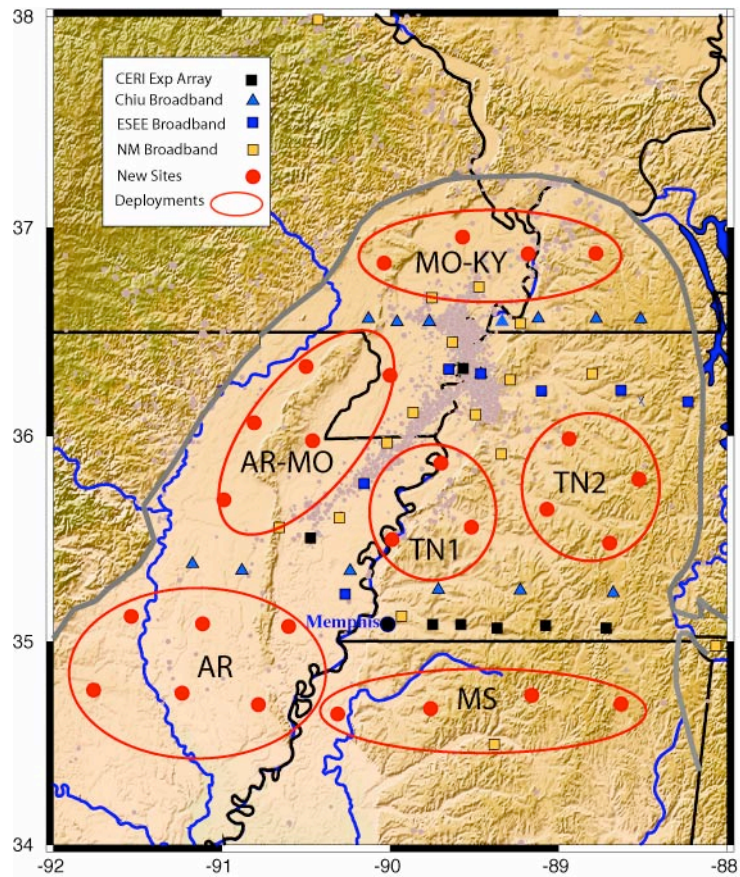

Figure 1 – Index map of the area showing the location of existing broadband seismic stations, locations of stations associated with special experiments available to the P.I.s, and new deployments for this project. The elliptical areas enclose broadband sites that will deployed in separate field efforts. The thick grey line shows the limit of Mississippi embayment unconsolidated sediments. Grey dots show the locations of recent earthquakes in the NMSZ.

Introduction

A variety of field studies have shown that Nakamura's (*Nakamura*, 1989) empirical technique for estimating shear wave site resonance frequencies is a robust method that can yield useful information about the structure of a site in the near-surface that may be used for shaking hazards assessments (*Lermo and Chavez-Garcia*, 1993; 1994; *Theodulidis and Bard*, 1995; *Bour et al.*, 1998; *Field et al.*, 1994; *Field and Jacob*, 1995; *Malagnini et al.*, 1996; *Lozano et al*., 2008; *Hagshenas et al*., 2008). The method employs three-component recording of ambient ground motions for a site of interest and then forms the ratio of the amplitude or power spectra of horizontal component ground motions (H) to the vertical component ground motions (V). The H/V ratio usually displays a set of peaks in ground motion that are interpreted in terms of the resonance of vertically incident shear waves in a simple layered velocity structure. The method is purely empirical and based on a set of intuitive assumptions about the wave propagation involved in ambient ground motions. In particular, the H/V ratio is interpreted in terms of a simple spectral transfer function where equal amplitude horizontal and vertical wave motions at depth are separately affected by the intervening structure on their way to the free surface. The major assumption is that shear waves are horizontally polarized and will be amplified by the usual decrease in shear wave

impedance in the near surface and will also resonate within the layered structure. The amplitude of the vertical wave field is assumed to be unaffected.

Theoretical studies using distributions of surface noise sources have shown that heterogeneous ambient noise fields do yield synthetic results for plane-layered velocity models consistent with Nakamura's assumptions (*Field and Jacob*, 1993; *Lachet and Bard*, 1994) and consistent with the propagation of Rayleigh and Love surface waves (*Konno and Ohmachi*, 1998). Nakamura (1989) also checked his basic assumption on the nature of vertical motions using borehole seismic observations. The frequencies of spectral peaks in the H/V ratio seems to be a robust feature that can be related to site structure but it is less clear if the amplitude of the peak is a useful measure of absolute ground motion amplification (*Lachet and Bard*, 1994).

Recently, we completed a study of the wave propagation mechanisms important for forming the H/V ratio in the Mississippi embayment (Langston et al. 2009). Ambient ground motion data were collected using phased seismic arrays in Fall 2002 and Spring 2007 within the Mississippi embayment and at a single station external to the embayment. These data allowed us to determine the wave field composition of ambient noise for understanding wave propagation mechanisms giving rise to spectral peaks using Nakamura's H/V technique. Ambient ground motions in the frequency band of 0.1 to 0.33 Hz (10 to 3 sec period) were dominated by spatially localized Rayleigh and Love wave microseisms generated by high ocean waves along the North American seaboard in the time periods of analysis. Seismic waves important in forming the H/V peak near 4 s period were composed of relatively high phase velocity Rayleigh and Love waves that convert to propagating homogeneous shear waves in the thick unconsolidated sediments of the embayment. The H/V resonant period was controlled by both constructive and destructive interference of these shear waves. A simple relationship for the H/V peak was given using a propagator matrix formulation that predicts the resonance frequency of a layered medium for surface wave motion at the base of the system. We found that the amplitude of the observed H/V peak, however, did not give an accurate estimate of shear wave amplification since it depends on the slowness of the incident wave. We also found that the inconsistency in estimated average shear wave velocities using the H/V method and differential travel times of local earthquake Sp phases in the Mississippi embayment could be explained by misidentification of Sp wave conversion points from deeper interfaces.

Based on these results, we believe that we understand the wave propagation mechanisms responsible for forming the H/V ratio in this period range from ambient noise fields generated in the North Atlantic. Interpretation of the H/V resonance period yields an estimate of the average shear wave velocity in the sediment column given knowledge about the sediment thickness at the site.

H/V Wave Propagation Mechanisms in the Mississippi Embayment

The Mississippi embayment (Figures 1 and 2) overlies the NMSZ in the central United States and consists of a thick succession of unconsolidated coastal plain sediments arranged in a shallow synformal structure (*Stearns*, 1957; *Stearns and Marcher*, 1962). The average shear

wave velocity of the sediments is approximately 700 m/s (*Langston*, 2003a) and thicknesses of up to a kilometer in the area predict low frequency site resonance effects. *Bodin and Horton* (1999) and *Bodin et al.* (2001) showed that H/V peak periods varied from about 3 to 5 seconds and that period correlated with sediment thickness.

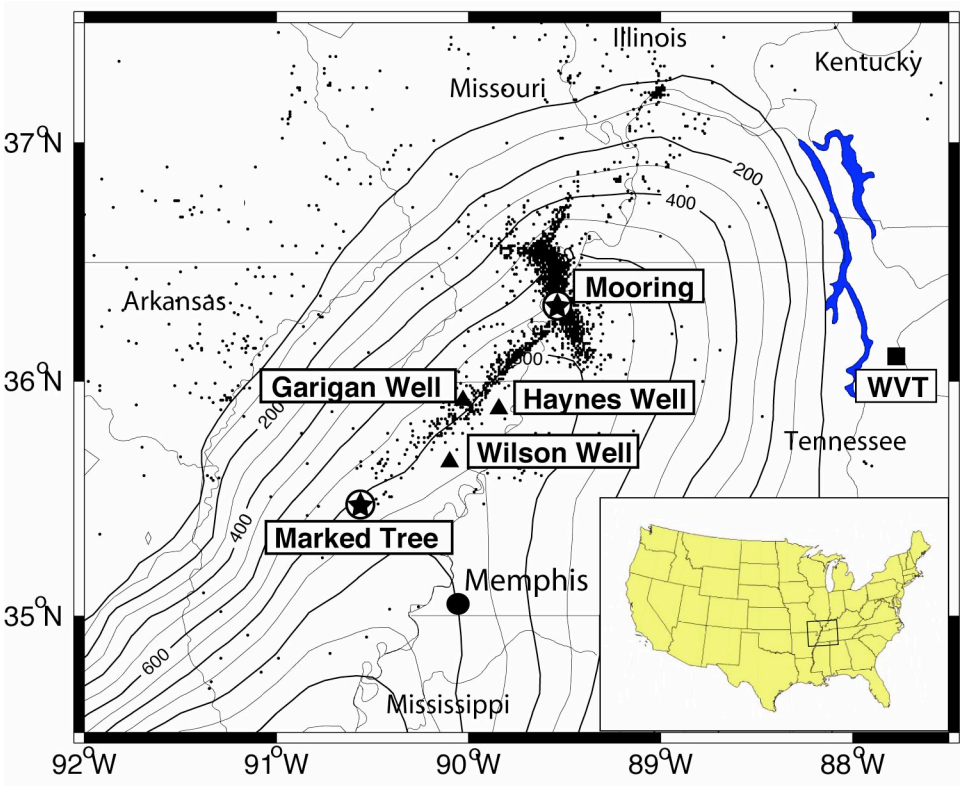

Figure 2 – Sediment thickness map (contours in meters) based on Dart and Swolfs (1998) with the location of phased arrays at Mooring, TN, and Marked Tree, AR. Locations of 3 deep wells are shown by the triangles. Waverly, TN, (WVT) station was used as a control station for the H/V array study.

Using constraints on sediment thickness from well log and reflection seismology depth estimates (*Dart*, 1992; *Dart and Swolfs*, 1998) Bodin et al. (2001) also found that the average shear wave velocity inferred from the resonant period increased with sediment thickness throughout the embayment (Figure 3). However, they pointed out that the average velocity estimates obtained from H/V measurement interpretations were significantly higher than that obtained from the interpretation of S-Sp differential travel times (*Chen et al.*, 1996). The Sp phase is a common observation on local earthquake seismograms in the NMSZ, and because it is so large, has been attributed to the large velocity contrast between the unconsolidated sediments and the underlying high-velocity Paleozoic limestones (*Andrews et al.*, 1985; *Chen et al.*, 1996; *Langston*, 2003b). Langston et al. (2009) found that much of the bias in velocity probably comes from misidentifying Sp phases that are generated at deeper interfaces within the Paleozoic section with those generated at the Paleozoic/Upper Cretaceous boundary at the base of the unconsolidated sediments. Thus, the H/V analysis gives a better estimate of sediment velocity than interpretation of Sp phase travel times.

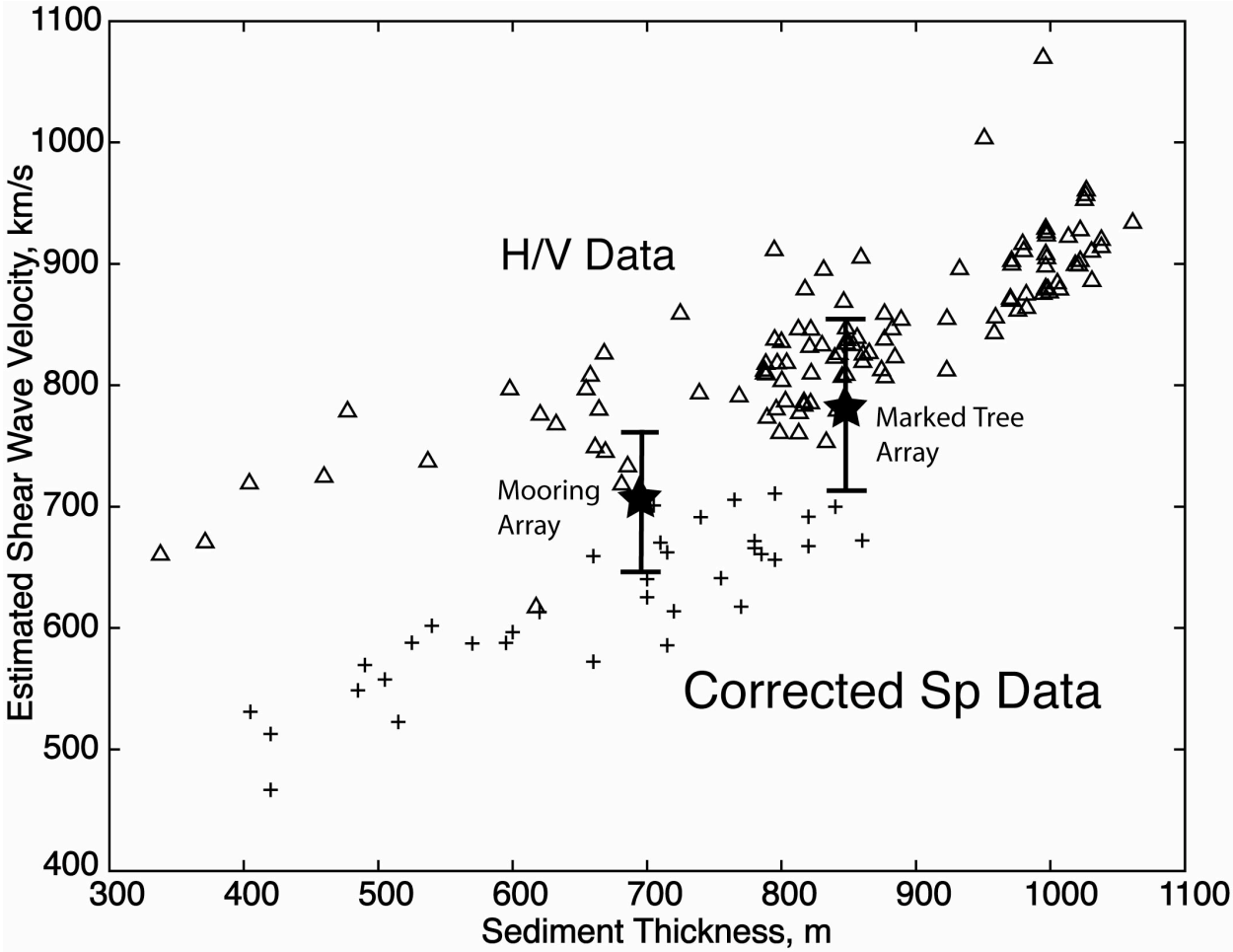

Figure 3 - Estimated shear wave velocity versus sediment thickness from interpretation of H/V spectral peaks (triangles) from Bodin et al (2001) and S-Sp travel times (crosses) from Chen et al (1996). The S-Sp travel time data were corrected by using an average P wave velocity of 2.1 km/s rather than Chen et al's (1996) value of 1.8 km/s based on a study of velocity structure by Langston (2003a). This serves to bring the H/V and Sp data results somewhat closer together. However, the two fields of points are still clearly separated and show an inconsistency explained through misidentification of deeper Sp phases. The stars show average velocities inferred from Mooring array data (at 700m sediment thickness) and Marked Tree array data (at 800m sediment thickness). Error bars for these estimates are based on a conservative estimate of the half-width of the H/V peak as $\pm$0.02 Hz.

Langston et al. (2009) used broadband phased arrays of seismometers to record ambient ground motions within the embayment. We used the array observations to perform a wave field decomposition to determine horizontal phase velocities and azimuths of the ambient noise to determine the source of the noise and wave types involved. The array data were processed using standard frequency-wavenumber beam forming techniques (e.g., *Nawab et al.*, 1985) and, for one array, using newly developed techniques of wave gradiometry (*Langston and Liang*, 2008). H/V ratios formed using the array data were then compared to ratios computed from a station outside of the embayment (Waverly, TN – WVT, Figure 2) to understand how the embayment amplifies ambient ground motions.

We found that ambient ground motions in the period band of 3-5 sec were spatially coherent and were caused by high ocean wave motions along the North Atlantic seaboard of North America. Figure 4 shows a rendering of the global WaveWatch III model available from the WaveWatch NOAA website. The array data at Mooring and Marked Tree showed that long period ambient ground motions consisted of high velocity (~3 km/s) Rayleigh and Love waves from northeastern azimuths, correlating with areas of high wave height. This observation was crucial to the analysis of the ambient noise because we could then know the parameters of the principal source waves that propagate into the embayment and interact with the thick unconsolidated sediments. We could then make appropriate wave propagation models to explain first order features of the H/V observations.

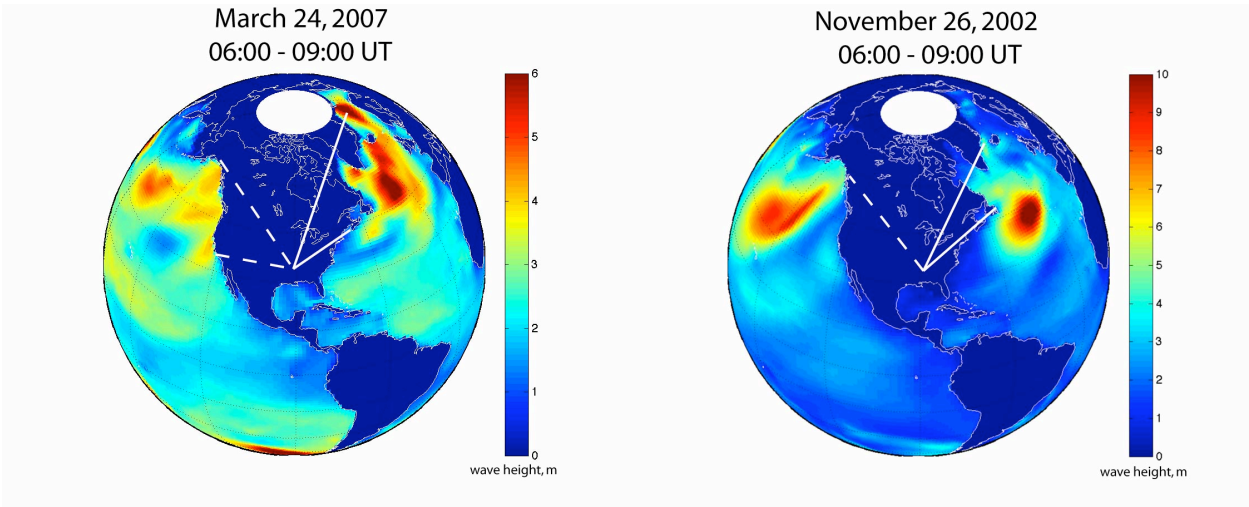

Figure 4 – Ocean wave heights from the WAVEWATCH III hindcast models published by NOAA (Tolman, 2005) for the data time periods used from the Marked Tree and Mooring array experiments. The solid white lines show the general azimuth directions inferred from the width of the frequency-wave number array response and gradiometry analyses for the frequency band 0.2-0.25Hz. The dotted lines are directions to high wave sources along the western margin of North America. Northeastern sources are only seen in the array data. Observed seismic waves were generated by storm-generated surf along the coasts of northeastern North America. Note that the important parts of the wave height model pertaining to the generation of ambient seismic noise are concerned with waves near the coasts. High waves offshore, such as for the 2002 time period, are not effective in generating seismic noise.

Figure 5 shows the computed H/V ratios at the two seismic arrays and at WVT station. H/V at WVT station, which is outside of the embayment, shows no spectral peak as expected. However, it is clear that amplification generally occurs for the horizontal components within the embayment. Even so, the H/V ratio within the embayment is affected by the vertical component motions since the peak of the H/V becomes well defined and is different from the peak of just the H motion alone. Figure 6 shows what happens to the surface wave train as it propagates into the embayment. H and V ratios of array to WVT motions demonstrate that significant amplification occurs in H due to the unconsolidated sediments, but V has a broad minimum near the H/V peak frequency.

These aspects of the data can be understood with simple upward continuation of a surface wave displacement field into a low velocity layer. Figure 7 shows a series of computations modeling the H/V peak for a low velocity layer over high velocity halfspace. The input motion at the base of the layer corresponds to a fundamental mode Rayleigh wave similar to what was observed in the array experiment. These model results show similar effects as seen in the observational data. H motions are significantly amplified but the V spectra control the exact placement of the H/V spectral peak because of its minimum. The minimum physically represents the change from retrograde to prograde particle motion at the surface. In effect, the frequency of the resonant peak is both controlled by amplification in H and a null in V. It was shown in Langston et al. (2009) that this frequency is virtually the same as that expected for resonance of a vertically propagating shear wave in the layer, the usual interpretation made in the H/V literature. However, it is due to destructive interference of the vertical component of motion for non-vertically propagating shear waves in the layer. The reality is different than commonly assumed.

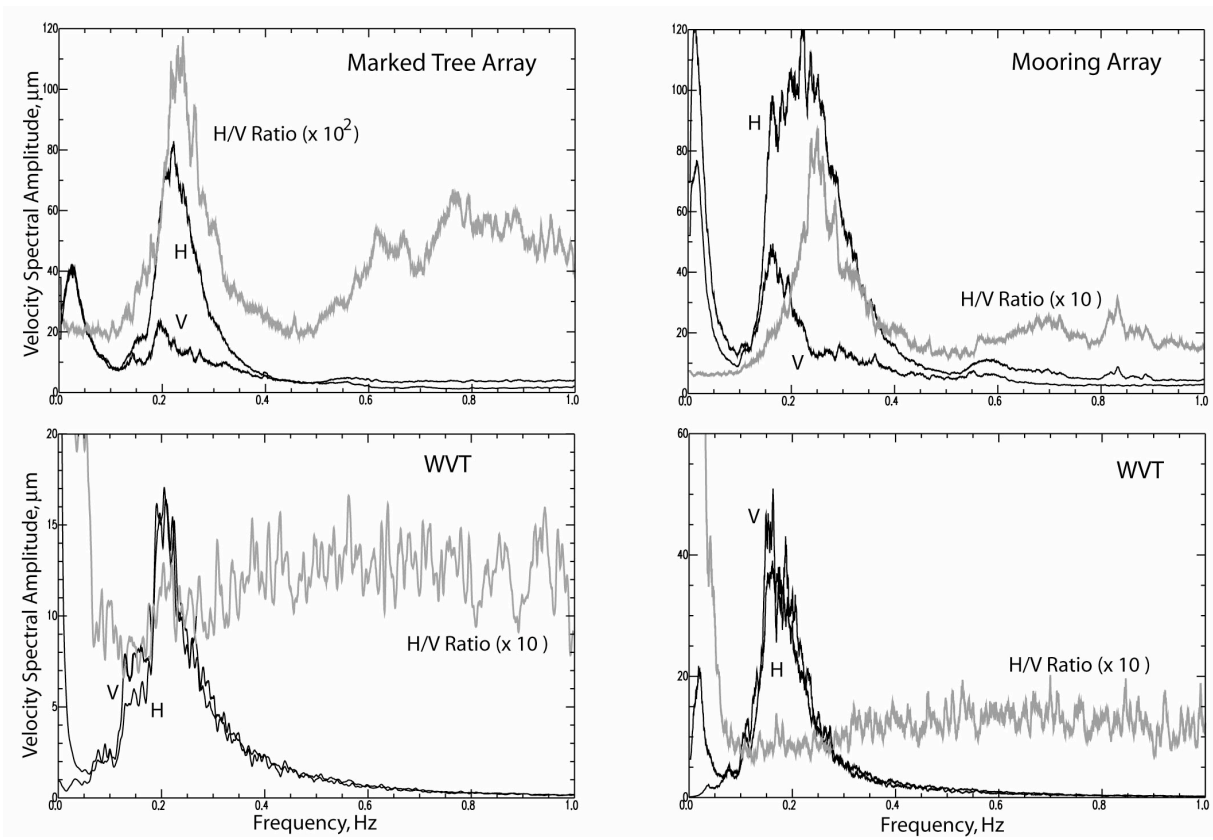

Figure 5 – Computed H amplitude spectra, V amplitude spectra, and H/V ratios for the pass band between 0 and 1 Hz for data recorded at the arrays and simultaneously at WVT station. One hour of data were used to compute the spectra. Data for the Marked Tree array were from 06:00 UT on 24 March 2007 and for the Mooring array from 08:00 UT on 26 November 2002. The H/V ratios have been multiplied by factors shown in the plots to enable comparison with the original H and V spectra. It should be understood that the H/V spectra have no units even though we are using the spectral amplitude scale in each plot.

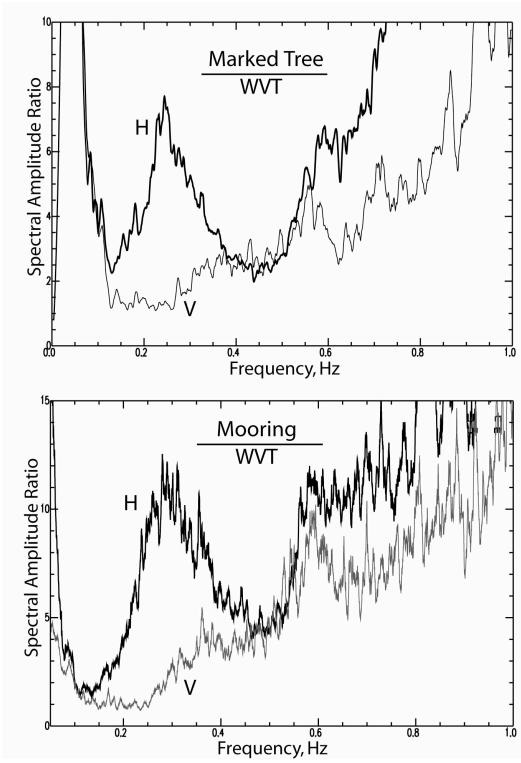

Figure 6 – H and V spectral ratios of array data to data from WVT station.

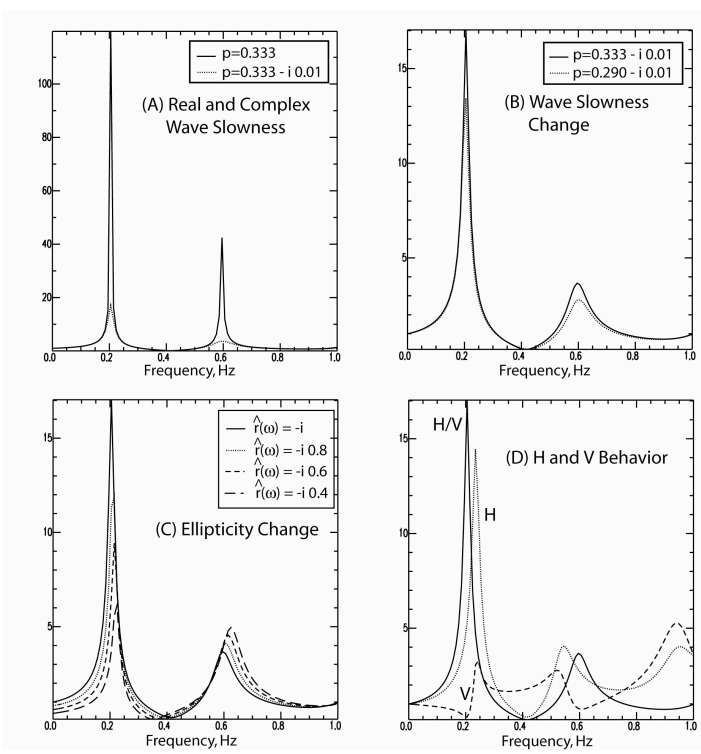

Figure 7 – A series of computations showing the upward continuation of Rayleigh wave motion to the surface of a low velocity layer (Vp=2.1 km/s, Qp=200, Vs=0.7 km/s, Qs=100, density=2.1 gm/cc, thickness=850 m) from a halfspace (Vp=6.1 km/s, Vs=3.5 km/s, density=2.7 gm/cc). Panel (A) show the effect of assuming complex horizontal slowness *p* to mimic Rayleigh wave geometrical spreading and attenuation. Peak height is reduced to values similar to that seen in the H/V data but the frequency of the peak is not affected. Panel (B) shows that the slowness of the incident Rayleigh wave does

not significantly affect the amplitude or frequency of the resonant peak. Panel (C) shows the effect of differing assumed ellipticities for the incident Rayleigh wave. The location of the resonant peak does change as well as its amplitude but this change is not large. Panel(D) shows details of the H and V spectra and the resulting H/V ratio (same display scheme as Figure 5). Although upward continuation produces a clear peak in the H spectra, it is the null in the V spectra that primarily controls the location of the H/V spectral peak.

Knowledge of the wave mechanism that gives rise to the H/V resonant peak also yields insight into the meaning of the peak amplitude. Because the input motion is a surface wave, the wave is an inhomogeneous, or evanescent, wave that decays with depth in the lower halfspace. However, the boundary condition requires that horizontal phase velocity be continuous (Huygen's principle) so that the Rayleigh wave converts into steeply propagating P and S waves within the layer. These P and S waves are totally trapped because, by definition, they have post-critical incidence angles at the lower layer boundary. The upward continuation computations shown in Figure 7 incorporate complex horizontal slowness that can be shown to mimic the effect of geometrical spreading and attenuation for a propagating Rayleigh wave. Without anelasticity, the spectral H/V peak would have infinite amplitude. Using a complex slowness produces amplitudes in line with the data. In any case, the amplitude is more a function of having waves totally trapped in the layer. It is easy to show that amplification for shear waves with horizontal slowness appropriate for local earthquake propagation would have much less amplification compared to the values of 12 and 8 seen in the data (Figure 5). Thus, the amplitude of the H/V peak is not a good proxy for amplification of earthquake shear waves.

Field Program

Ambient noise data were collected from 29 new sites within the northern Mississippi embayment. General site locations were picked from maps with the goal to have a well-distributed pattern of seismic station locations. Approximately 5 to 6 sites could be visited in a day. The specific site was found by driving around in the general chosen site area, which was always rural, and finding out-of-way and/or unused farm fields where the seismometer could be emplaced by the fence row away from main roads. A small hole was dug using a posthole shovel and the seismometer placed in the hole, oriented, and secured with loose soil and sand. A paving tile would be placed on top of the hole to reduce wind noise and exposure to the sun. Recording would last from 15 to 20 minutes and would be carefully and quietly monitored to make sure the seismometer was functioning with a minimum of the usual long-period transients induced by jolting during installation. After data collection, the data would undergo rough processing to make sure an H/V peak was observed.

Other Broadband Data

Data segments were also obtained for particular times from several past broadband field experiments in the embayment and from broadband stations of the New Madrid Cooperative Seismic Network (Figure 1). Unlike the field program, which occurred in the daytime, we chose ambient noise data in the night time where cultural noise would be at a minimum. It was noted that this data set was generally much higher quality than the data from the field campaign.

H/V Processing

A MatLab Graphical User Interface (GUI) was written to efficiently process the data (Figure 8). Whenever possible, a least 600 s (10 minutes) of three component data were used in the analysis at each station. Data are read into the GUI then time windowed, the mean or quadratic trend removed, and tapered with a 10% cosine window taper. The power spectrum of the vertical component and the square root of the sum of the squares of the horizontal components were then computed. The power spectra were smoothed with a 21-point running average and the H/V spectral ratio computed.

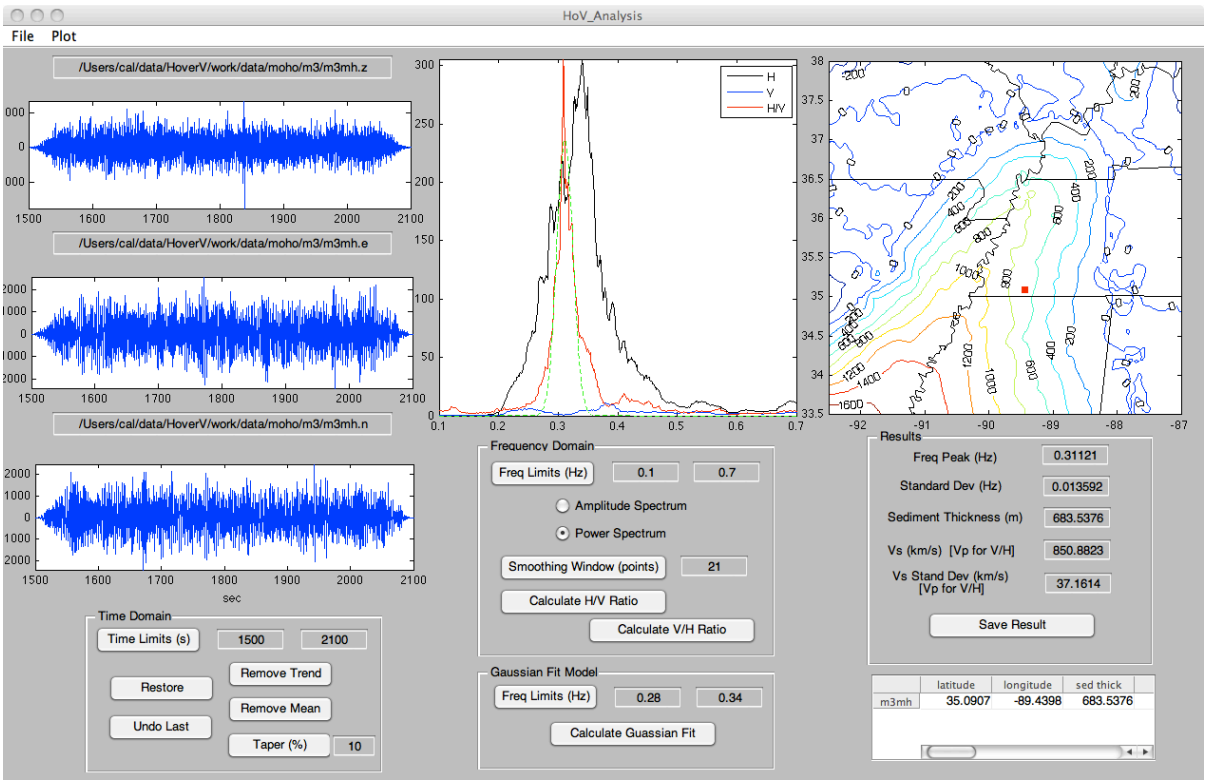

Figure 8 – Screen capture image of the GUI. The left column and menu items are concerned with reading in the basic waveform data, removing the signal mean or a trend and tapering before the FFT. The central section displays the power (or amplitude) spectra and the H/V spectral peak. Usually, a 21-point smoothing operator was applied to the power spectra before taking the ratio. A Gaussian function was then fit to the H/V frequency peak by computing the first and second moments of the H/V peak between chosen frequency limits and assigning the first moment to be the mean and second moment the variance of a Gaussian distribution. The Gaussian is shown in green. The right side displays the resulting estimates of sediment thickness and errors that are saved in a table and ultimately saved to a file.

The H/V peak was chosen on the amplitude-frequency plot rather than the amplitude-period plot. This was done for the simple reason that the shear-wave velocity, v_s, is directly proportional to the frequency, f_P, of the H/V peak through the classic relation

$$v_s = 4hf_P \qquad (1)$$

where h is the sediment layer thickness. Because this relation is linear, error in picking f_P, say σ_f, gives a linear relation for the error in v_s, σ_v,

$$\sigma_v = 4h\sigma_f \quad . \qquad (2)$$

The error in f_P was computed by calculating the first and second moments of the peak, choosing integration bounds that ensured that the peak of a Gaussian function coincided with the data H/V peak. Essentially, a Gaussian distribution function was fit to the data. The resulting standard deviation, σ_f, represents peak width that translated into velocity uncertainty through equation (2).

The GUI also interpolated the sediment thickness map to assign a value of thickness to each station location. This thickness was then used in equations (1) and (2) to compute shear-wave velocity and its standard deviation. Results were saved in a table and then output to a file for further analysis.

A total of 61 stations (Figure 9) where used in this study. Three stations near the edge of the embayment were not used because of poor data quality or because it was very difficult to pick an appropriate H/V peak.

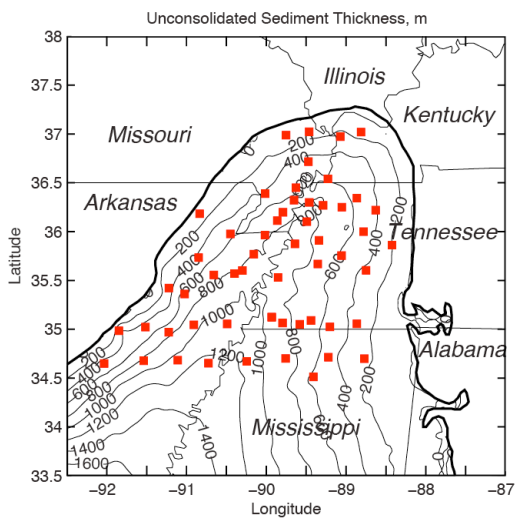

Figure 9 – Location of the stations used in this study. These stations consist both of new field stations, broadband stations deployed in special experiments, and broadband stations of the New Madrid Cooperative Seismic Network.

Data Systematics

We obtained similar results for H/V frequency peak systematics as found in past studies. A plot of peak period versus sediment thickness appears to be linear, at least for sediment thickness greater than 200 m (Figure 10a) similar to results found by Bodin and Horton (1999) and Bodin et al. (2001). H/V peaks for stations on thinner sediments often were spectacular, but some stations were ambiguous showing multiple peaks or very broad peaks. As a result, some data for h < 200m give very low, unrealistic shear-wave velocities. These data were not modeled in the following.

If the period-thickness relation is linear then, by equation (1), the velocity-thickness relation cannot possibly be linear. Thus, combining a linear frequency-thickness relation with a linear velocity-thickness relation is not a self-consistent model, even though a line can be fit to the velocity-thickness data (Figure 10d). Plotting peak frequency versus thickness bears this out (Figure 10b) but still looks deficient for data associated with 200-300m sediment thickness. Plotting the natural log of the peak frequency versus sediment thickness should produce a straight line if period versus thickness is truly linear. However, the data show that there is noticeable curvature in the distribution that warrants fitting $ln\, f_P - h$ with a quadratic function (Figure 10c). This yields the principal result of this research project

$$\ln f = 1.038 \times 10^{-6} h^2 - 0.0026411 h + 0.10108 \qquad (3)$$

giving

$$v_s = 4he^{\ln f} \quad . \qquad (4)$$

The shear-wave velocity versus thickness plot shows smooth variation through the data, lies close to the linear fit line but predicts lower velocities for thickness less than 400m and higher velocities for thickness greater than 1000m (Figure 10d).

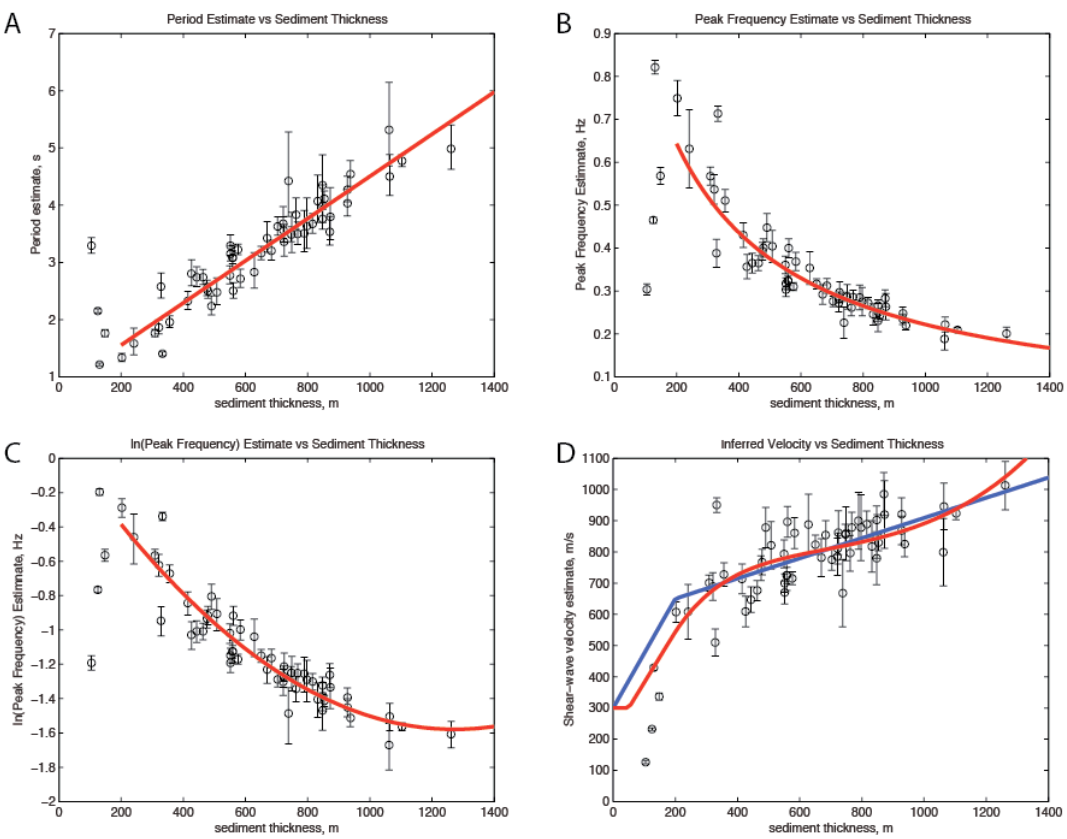

Figure 10 – (A) H/V peak period vs sediment thickness with linear fit. (B) H/V peak frequency vs sediment thickness with the predicted curve from the linear fit in (A), The prediction underfits for data with sediment thickness less than 300m. (C) Natural logarithm of the peak frequency vs sediment thickness with a quadratic line fit. (D) Fit of the velocity – sediment thickness estimates using a straight line (blue) and the implied peak frequency – velocity fit through equation (1). The fits used data for 200-1300m thickness. Velocity is assumed for thickness less than 200m.

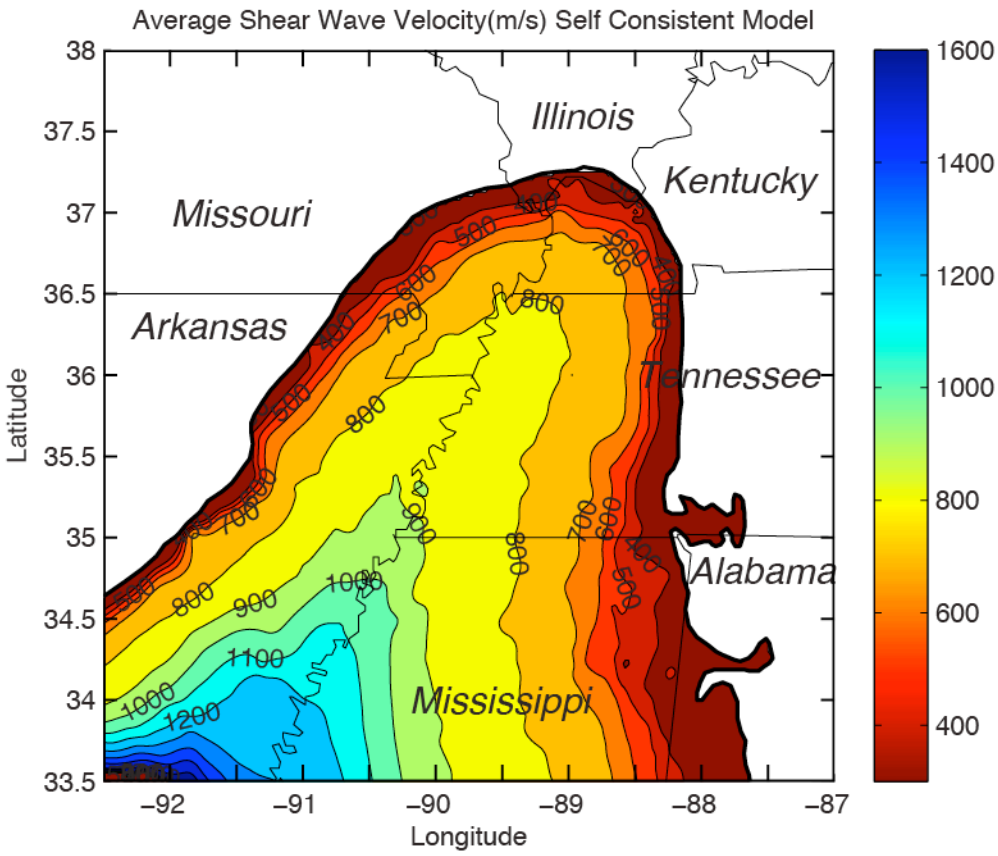

Figure 11 – Average velocity for the unconsolidated sediments of the Mississippi embayment using the self-consistent model, equations (3) and (4). Shear-wave velocity in m/s.

Average Sediment Velocity Maps

Armed with this relationship, it is a straightforward task to translate the sediment thickness map into a map of average shear-wave velocity (Figure 11). Because we do not have sufficient data to characterize the thinnest sediments around the edge of the embayment, we simply linearly extend the velocity-thickness relation to 50m where a constant velocity of 300 m/s is assumed for the thinnest sediments (Figure 10d).

Comparing the self-consistent model map (Figure 11) with that of a map constructed using the theoretically inconsistent linear model (Figure 12) shows that there are minor differences for sediment thickness from 300 to 1000m. The self-consistent model predicts lower average velocities from 200-300m thickness and higher for thicknesses greater than 1000m.

Although theoretically pleasing, clearly this is only an empirical result that can be tested with more H/V data in the deeper portions of the embayment.

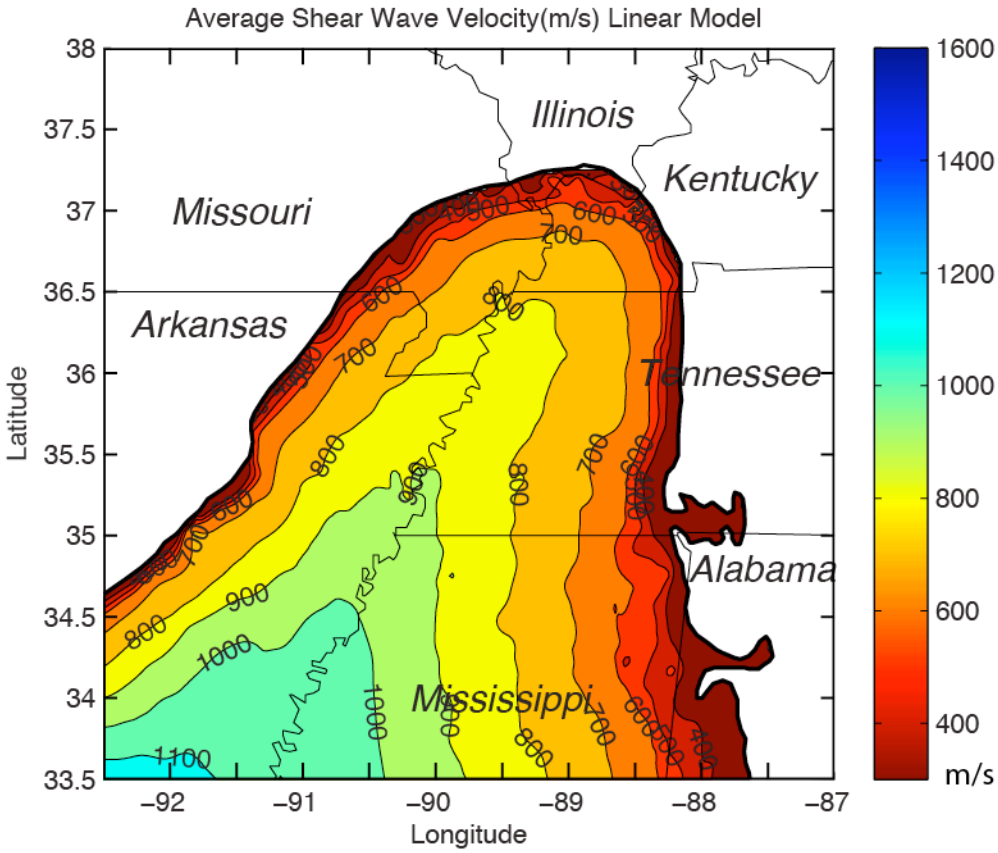

Figure 12 – Average shear-wave velocity map of the Mississippi embayment using the linear velocity-thickness relation shown in Figure 10d. Shear-wave velocity in m/s.

Discussion

We were initially concerned with choosing data that were generated by a northeast-situated ambient noise source to produce ground motions consistent with what we saw in the published array study. A perusal of WaveWatch III models (Figure 13) for the data analyzed here always showed high wave areas in the northern Atlantic basin that presumably are the source of microseisms recorded in the embayment (Langston et al., 2009).

However, Langston et al. (2009) also point out that ambient noise sources become complex for periods approaching 1s. Waves at 1 Hz may propagate more as shear waves (as in the Lg phase) than standard surface waves. So, waves producing the H/V peak at 0.5 to 1 Hz may have different resonant characteristics than ambient noise surface waves at 0.2-0.25Hz. Generally, this will mean that the sediment waveguide will be leakier allowing resonating shear waves in the sediment to loose energy faster. This causes an effective Q, broadening

the H/V peak and lowering the peak frequency. This could be the cause of the erratic data seen for stations located on thin sediments.

The 3-D map (Figure 11) suggests that horizontally propagating surface waves will tend to refract towards the center of the embayment, particularly if they are propagating from the north. It remains to be seen how this velocity structure affects strong ground motion simulations for sources outside and inside the embayment (e.g., Ramirez-Guzman et al., 2009). At a minimum, this velocity model is simple, testable with more and different data, and can serve as a first-approximation for the overall velocity structure of the unconsolidated embayment sediments.

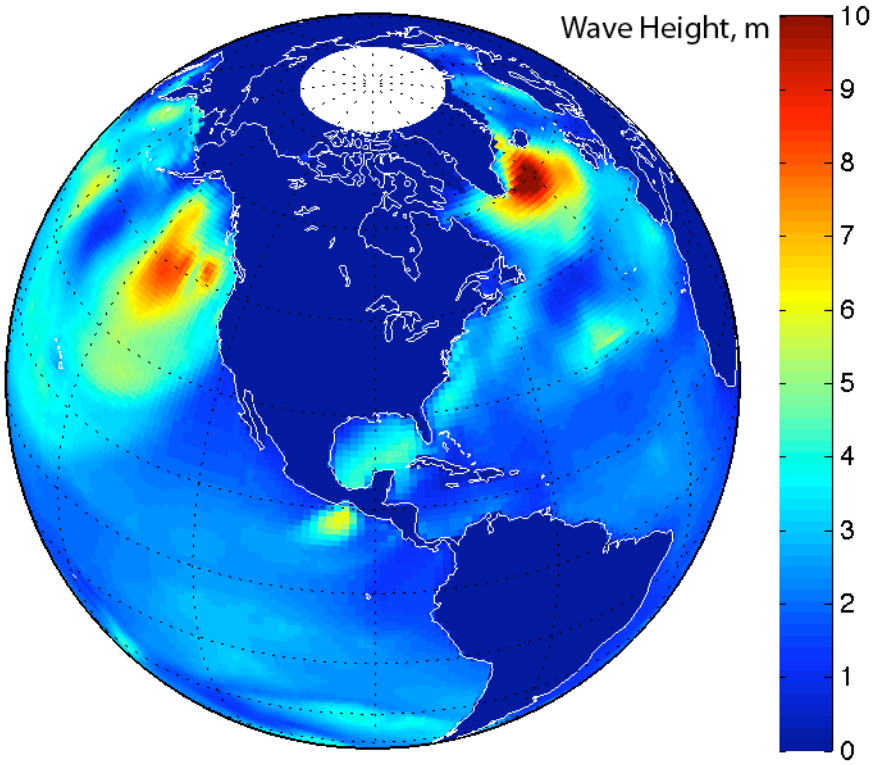

Figure 13 – WaveWatch III model for March 2, 2009 at 0900 UTC appropriate for data used from the CERI "Moho" seismic experiment located near the Tennessee-Mississippi border. Wave heights (in m) are similar to that shown in Figure 4 where it was observed that ambient noise surface waves propagated from the northeast azimuth, implying that storms in the North Atlantic are the source for most of the ambient ground motions in the embayment area.

DISPOSITION OF DATA SETS

The terms of this grant requires that all data be made freely available to other investigators. All data are available by request. Some data are available at the IRIS data center.

BIBLIOGRAPHY OF ALL PUBLICATIONS RESULTING FROM THIS PROJECT

None at this time. A paper is currently being prepared.

ACKNOWLEDGMENTS

CERI graduate students Mehari Ayele, Blaine Bockholt, and Paul Ogwari participated in the fieldwork for this project and are acknowledged for their help.

REFERENCES

Andrews, M. C., W. D. Mooney, and R. P. Meyer (1985). The relocation of microearthquakes in the northern Mississippi embayment, *Jour. Geophys. Res.*, *90*, 10223-10236.

Bodin, P., and S. Horton (1999). Broadband microtremor observation of basin resonance in the Mississippi embayment, central U.S.: Implications for seismic hazard assessment, *Geophys. Res. Lett.*, *26*, 903-906.

Bodin, P., K. Smith, S. Horton, and H. Hwang (2001). Microtremor observations of deep sediment resonance in metropolitan Memphis, Tennessee, *Engin. Geol.*, *62*, 159-168.

Bour, M., D. Fouissac, P. Dominique, and C. Martin (1998). On the use of microtremor recordings in seismic microzonation, *Soil Dynamics and Earthquake Engineering*, *17*, 465-474.

Chen, K., J. Chiu, and Y. Yang (1996). Shear-wave velocity of the sedimentary basin in the upper Mississippi embayment using S-to-P converted waves, *Bull. Seism. Soc. Am.*, *86*, 848-856.

Dart, R. L. (1992). Catalog of pre-Cretaceous geologic drill-hole data from the upper Mississippi embayment: a revision and update of open-file report 90-260, U. S. Geological Survey Open-File Report 92-685.

Dart, R. L., and H. S. Swolfs (1998). Contour mapping of relic structures in the Precambrian basement of the Reelfoot rift, North American midcontinent, *Tectonics*, *17*, 235-249.

Field, D. H., and K. H. Jacob (1993). The theoretical response of sedimentary layers to ambient seismic noise, *Geophys. Res. Lett.*, *20*, 2925-2928.

Field, D. H., and K. H. Jacob (1995). A comparison and test of various site response estimation techniques, including three that are non-reference-site dependent, *Bull. Seism. Soc. Am.*, *85*, 1127-1143.

Field, E. H., A. C. Clement, K. H. Jacob, V. Aharonian, S. E. Hough, P. A. Friberg, T. O. Babaian, S. S. Karapetian, S. M. Hovanessian, and H. A. Abramian (1994). Earthquake site-response study in Giumri (formerly Leninakan), Armenia, using ambient noise observations, *Bull. Seism. Soc. Am.*, *84*, 349-353.

Haghshenas, E., P.-Y. Bard and N. Theodulidis, SESAME WP04 Team (2008). Empirical evaluation of microtremor H/V spectral ratio, *Bull Earthquake Eng,* **6** , 75–108 10.1007/s10518-007-9058-x.

Konno, K., and T. Ohmachi (1998). Ground-motion characteristics estimated from spectral ratio between horizontal and vertical components of microtremor, *Bull. Seism. Soc. Am.*, *88*, 228-241.

Lachet, C., and P.-Y. Bard (1994). Numerical and theoretical investigations on the possibilites and limitations of Nakamura's technique, *J. Phys. Earth*, *42*, 377-397.

Langston, C. A. (2003a). Local Earthquake Wave Propagation Through Mississippi Embayment Sediments: I. Body Wave Phases and Local Site Responses, *Bull. Seism. Soc. Am.*, *93*, 2664-2684.

Langston, C. A. (2003b). Local earthquake wave propagation through Mississippi embayment sediments: II. Influence of local site velocity structure on Qp-Qs determinations, *Bull. Seism. Soc. Am.*, *93*, 2685-2702.

Langston, C. A., and C. Liang (2008). Gradiometry for polarized seismic waves, *Jour. Geophys. Res.*, doi:10.1029/2007JB005486, in press.

Langston, C.A., S.-C. Chi Chiu, Z. Lawrence, P. Bodin, and S. Horton (2009). Array observations of microseismic noise and the nature of H/V in the Mississippi embayment, *Bull. Seism. Soc. Am.*, in press.

Lermo, J., and F. J. Chavez-Garcia (1993). Site effect evaluation using spectral ratios with only one station, *Bull. Seism. Soc. Am.*, *83*, 1574-1594.

Lermo, J., and F. J. Chavez-Garcia (1994). Site effect evaluation at Mexico City: dominant period and relative amplification from strong motion and microtremor records, *Soil Dynamics Earthquake Eng.*, *13*, 413-423.

Lozano, L., M. Herraiz, and S.K. Singh (2008). Site effect study in central Mexico using H/V and SSR techniques: Independence of seismic site effects on source characteristics, *Soil Dyn. Earth. Eng.*, 29, doi:10.1016/J.soildyn.2008.05.009, 504-516.

Malagnini, L., P. Tricarico, A. Rovelli, R. B. Herrmann, S. Opice, G. Biella, and R. de-Franco (1996). Explosion, earthquake, and ambient noise recordings in a Pliocene sediment-filled valley; influences on seismic response properties by reference- and non-reference-site techniques., *Bulletin of the Seismological Society of America.*, *86*, 670-682.

Nakamura, Y. (1989). A method for dynamic characteristic estimation of subsurface using microtremor on the ground surface, *QR Railway Tech. Res. Inst.*, *30*.

Nawab, S., F. Dowla, and R. Lacoss (1985). Direction determination of wideband signals, *IEEE Trans. Acous. Speech Sig. Proc.*, *33*, 1114-1122.

Ramirez-Guzman, L., Williams, R.A., Boyd, O., Hartzell, S., Earthquake Ground Motion Simulations in the Central United States, SSA annual meeting 2009.

Romero, S., and G.J. Rix (2001) Regional variations in near surface shear wave velocity in the greater Memphis area, Engin. Geol., 62, 137-158,

Stearns, R. G. (1957). Cretaceous, Paleocene, and lower Eocene geologic history of the northern Mississippi embayment, *Geol. Soc. Am. Bull.*, *68*, 1077-1100.

Stearns, R. G., and M. V. Marcher (1962). Late Cretaceous and subsequent structural development of the northern Mississippi embayment area, *Geol. Soc. Am. Bull.*, *73*, 1387-1394.

Theodulidis, N. P., and P.-Y. Bard (1995). Horizontal to vertical spectral ratio and geological conditions: an analysis of strong motion data from Greece and Taiwan (SMART-1), *Soil Dynamics and Earthquake Engineering*, *14*, 177-197.

Tolman, H. L. (2005). Manual and wave user system documentation of WAVEWATCH-III, ver. 2.22, 133 pp. pp, Washington, D.C., (Available at http://polar.ncep.noaa.gov/waves/wavewatch/wavewatch.html).